

# Supporting Information

Li et al. 10.1073/pnas.0808880106

## SI Methods

**Chemicals and Instruments.** Adenosine triphosphate disodium salt (ATP), CoA, flavin adenine dinucleotide disodium salt (FAD),  $\beta$ -nicotinamide adenine dinucleotide reduced disodium salt (NADH), (*R*)-1-phenyl-1,2-ethanediol, (*R*)-2-amino-1-phenyl-1-ethanol, (*R*)-2-phenylglycinol, and Tris(2-carboxyethyl)phosphine hydrochloride (TCEP) were purchased from Sigma-Aldrich. DTT and isopropylthiogalactoside (IPTG) were purchased from Research Products International Corp.. (*S*)-3-amino-3-(4-hydroxyphenyl)-propionic acid [(*S*)- $\beta$ -tyrosine] and (*R*)-3-amino-3-(4-hydroxyphenyl)-propionic acid [(*R*)- $\beta$ -tyrosine] were from PepTech Corp.. Medium components and buffers were from Fisher Scientific. Synthetic DNA oligonucleotides were purchased from the University of Wisconsin, Madison Biotechnology Center (Madison, WI).

PCR was performed with a PerkinElmer GeneAmp 2400. Routine atmospheric pressure chemical ionization-mass spectroscopy (APCI-MS) was measured with an Agilent 1100 VL APCI Mass Spectrometer. Electrospray ionization-mass spectroscopy (ESI-MS) or high-resolution electrospray ionization-mass spectroscopy (HR-ESI-MS) was performed with an Agilent 1100 HPLC-MSD SL ion trap mass spectrometer (Agilent Technologies). High-resolution matrix-assisted laser desorption-ionization mass spectroscopy (HR-MALDI-TOF-MS) analysis was performed with a Varian ProMALDI (Varian Inc.). 1D and 2D NMR spectral data were recorded on Varian UI-500 spectrometers (Varian). HPLC analyses were carried out on a Varian HPLC system equipped with Prostar 210 pumps, a photodiode array detector, and an Appolo C18 reverse-phase column (5  $\mu$ m, 4.6  $\times$  250 mm; Alltech Associates Inc.) and using a mobile phase system that consisted of 0.1% trifluoroacetic acid (TFA) in milli-Q water (A) and 0.1% TFA in 90% acetonitrile/water (B).

**Bioinformatics Analysis of SgcC5.** Seventeen condensation domains and enzymes, including known or putative amide- and ester-forming condensation enzymes, were chosen from the literature. The multisequence alignment was performed with ClustalW2 using default parameters. The region containing the highly conserved motif (HHXXDX<sub>14</sub>Y) in condensation domains and enzymes is shown in Fig. S1, and the active sites are highlighted in red.

**Cloning, Overproduction, and Purification of SgcC5.** The *sgcC5* gene was amplified by PCR from cosmid pBS1005 (1, 2). PCR was performed with Platinum Pfx polymerase from Invitrogen using the following primers: forward 5'-GGT ATT GAG GGT CGC atg acg acg tcc gac acc a-3' and reverse 5'-AGA GGA GAG TTA GAG TCA GGA GGT GAA GGG GGC-3' (starting and stop codon italicized). The gel-purified PCR products were cloned into the pET-30 Xa/LIC vector by using ligation-independent cloning method as described by Novagen to give pBS1093 for *Escherichia coli* expression. Overexpression in *E. coli* BL21 (DE3) and purification of the recombinant SgcC5 protein by affinity chromatography using NTA-Ni agarose column (Qiagen) were performed following previously described procedures (3, 4). After the purified protein was desalted through a PD-10 desalting column (GE Healthcare) and concentrated with a Vivaspin ultrafiltration device [10,000 molecular-weight cut-off (MWCO); Sartorius], the SgcC5 protein was stored at -25 °C as a 40% glycerol stock. The purity of the purified protein was assessed by 12% SDS/PAGE (Fig. S2), and the concentration was determined from the absorbance at 280 nm by using a molar

absorptivity ( $\epsilon = 47.5 \text{ mM}^{-1}\text{cm}^{-1}$ ) calculated by using the program Protparam ([www.expasy.ch/tools/protparam.html](http://www.expasy.ch/tools/protparam.html)).

**Overproduction and Purification of SgcC, SgcC1, SgcC2, SgcC3, SgcE6, and Svp.** Production in *E. coli* and purification to homogeneity of SgcC (4), SgcC1 (5), SgcC2 (3), SgcC3 (3), Svp (6), and SgcE6 were carried out according to literature procedures by using affinity column chromatography. The concentrations of SgcC, SgcC1, SgcC2, and Svp were determined by using the program Protparam ([www.expasy.ch/tools/protparam.html](http://www.expasy.ch/tools/protparam.html)) based on their absorptivity at 280 nm. The concentrations of SgcC3 and SgcE6 were determined by using the Bradford protein assay (Bio-Rad).

**Enzymatic Synthesis of (*R*)-3-Chloro-5-Hydroxy- $\beta$ -Tyrosine and (*S*)-3-Chloro-5-Hydroxy- $\beta$ -Tyrosine Standards.** (*R*)-3-chloro-5-hydroxy- $\beta$ -tyrosine and (*S*)-3-chloro-5-hydroxy- $\beta$ -tyrosine were prepared enzymatically from (*R*)- $\beta$ -tyrosine and (*S*)- $\beta$ -tyrosine, respectively (Fig. S3A). First, apo-SgcC2 was converted to holo-SgcC2 by Svp in a 1.8 mL of reaction mixture containing 100 mM Tris-HCl (pH 7.5), 400  $\mu$ M apo-SgcC2, 2.0 mM CoA, 12.5 mM MgCl<sub>2</sub>, 2 mM TCEP, and 20  $\mu$ M Svp. After incubation at room temperature for 45 min, a loading mixture containing 7 mM (*S*)- $\beta$ -tyrosine, 10 mM ATP, 2 mM TCEP, and 12.5 mM MgCl<sub>2</sub> was added to an equal volume of the above solution. SgcC1 was added to a final concentration of 10  $\mu$ M, and the resulting solution was incubated at room temperature for additional 45 min to load (*S*)- $\beta$ -tyrosine to holo-SgcC2. The resultant (*S*)- $\beta$ -tyrosyl-(*S*)-SgcC2 was purified by using the anion-exchange chromatography following the procedure as described in our prior work (3). To obtain (*R*)- $\beta$ -tyrosyl-(*S*)-SgcC2, apo-SgcC2 was converted to holo-SgcC2 as described above. The holo-SgcC2 was incubated with the same loading mixture except that commercial (*R*)- $\beta$ -tyrosine (15 mM) and 15 mM ATP were used. After incubation at room temperature for 45 min, the proteins were removed from the loading mixture by centrifugation using a 4-mL centrifugal filter device (5,000 MWCO; GE Healthcare). The resulting 3.0 mL of filtrate was incubated with 200  $\mu$ M apo-SgcC2, 10  $\mu$ M Svp and 20  $\mu$ M SgcC1 at room temperature for an additional 45 min. (*R*)- $\beta$ -tyrosyl-(*S*)-SgcC2 was purified following the same procedure as for (*R*)- $\beta$ -tyrosyl-(*S*)-SgcC2. The purified (*S*)- $\beta$ -tyrosyl-(*S*)-SgcC2 and (*R*)- $\beta$ -tyrosyl-(*S*)-SgcC2 were concentrated by using a centrifugal filter device (5,000 MWCO; GE Healthcare) before use for subsequent enzymatic reactions.

(*R*)-3-chloro-5-hydroxy- $\beta$ -tyrosyl-(*S*)-SgcC2 and (*S*)-3-chloro-5-hydroxy- $\beta$ -tyrosyl-(*S*)-SgcC2 were made by a sequence of enzymatic reactions using SgcC3, SgcC, and SgcE6. The purified (*R*)- $\beta$ -tyrosyl-(*S*)-SgcC2 or (*S*)- $\beta$ -tyrosyl-(*S*)-SgcC2 was incubated with 100  $\mu$ M SgcC3, 20  $\mu$ M SgcE6, 0.3 M NaCl, 10 mM NADH, 100  $\mu$ M FAD, 1 mM TCEP, and 100 mM phosphate buffer (pH 6.0) at 30 °C for 3 h (3). The resultant (*S*)-3-chloro- $\beta$ -tyrosyl-(*S*)-SgcC2 or (*R*)-3-chloro- $\beta$ -tyrosyl-(*S*)-SgcC2 was purified through the same anion-exchange column. After concentration, the purified (*S*)-3-chloro- $\beta$ -tyrosyl-(*S*)-SgcC2 or (*R*)-3-chloro- $\beta$ -tyrosyl-(*S*)-SgcC2 was incubated with 10  $\mu$ M SgcC, 2  $\mu$ M SgcE6, 10 mM NADH, 20  $\mu$ M FAD, 1 mM TCEP, 0.1 M NaCl, and 20  $\mu$ M SgcC3 in 100 mM phosphate buffer (pH 6.0) (4). After incubation at 25 °C for 2 h, (*R*)-3-chloro-5-hydroxy- $\beta$ -tyrosyl-(*S*)-SgcC2 or (*S*)-3-chloro-5-hydroxy- $\beta$ -tyrosyl-(*S*)-SgcC2 was purified by anion-exchange column chromatography. The resultant acylated SgcC2 fraction was concentrated by using

a centrifugal filter device (5,000 WMCO), and the proteins were precipitated by addition of 70% cold trichloroacetic acid to a final concentration of 10%.

(*R*)-3-chloro-5-hydroxy- $\beta$ -tyrosine or (*S*)-3-chloro-5-hydroxy- $\beta$ -tyrosine was released from (*R*)-3-chloro-5-hydroxy- $\beta$ -tyrosyl-(*S*)-SgcC2 or (*S*)-3-chloro-5-hydroxy- $\beta$ -tyrosyl-(*S*)-SgcC2, respectively, as a free acid by incubating in an alkaline solution (0.1 M KOH) containing 50 mM DTT as described in ref. 4. (*R*)-3-chloro-5-hydroxy- $\beta$ -tyrosine and (*S*)-3-chloro-5-hydroxy- $\beta$ -tyrosine were purified by HPLC following the program used previously (4). The fractions were collected, and the removal of solvent was achieved by speed-vac. The resulting amino acids were redissolved in 50  $\mu$ L of perchloric acid buffer (pH 1.5) and analyzed with a CrownPak CR (+) column (5  $\mu$ m, 150  $\times$  4.0 mm; Chiral Technologies Inc.) to determine the stereochemistry (Fig. S3C). The column was developed under isocratic condition in aqueous perchloric acid buffer (pH 1.5) at a flow rate of 1 mL $\cdot$ min $^{-1}$  as recommended by the manufacturer.

**Chemoenzymatic Synthesis of (*S*)-3-Chloro-5-Hydroxy- $\beta$ -Tyrosyl-(*S*)-SgcC2.** First, racemic 3-chloro-5-hydroxy- $\beta$ -tyrosine was prepared according to previously reported procedure (4). Second, apo-SgcC2 was converted into holo-SgcC2 by incubating 1.8 mL of reaction mixture containing 100 mM Tris $\cdot$ HCl (pH 7.5), 400  $\mu$ M apo-SgcC2, 2.0 mM CoA, 12.5 mM MgCl<sub>2</sub>, 2.0 mM TCEP, and 20  $\mu$ M Svp at 25  $^{\circ}$ C for 45 min. Third, to this solution an equal volume of a loading solution consisting of 10 mM synthetic 3-chloro-5-hydroxy- $\beta$ -tyrosine, 10 mM ATP, 2.0 mM TCEP, and 12.5 mM MgCl<sub>2</sub> was added. SgcC1 was then added to a final concentration of 10  $\mu$ M, and the resulting solution was incubated at 25  $^{\circ}$ C for an additional 45 min. The SgcC2-tethered substrate was purified by using anion-exchange chromatography as described previously (3, 4). The purified substrate eluted between 0.35 and 0.4 M NaCl was concentrated by using a centrifugal filter device (5,000 MWCO; GE Healthcare) before use in SgcC5 assays. Fig. S3B depicts the chemoenzymatic synthesis of (*S*)-3-chloro-5-hydroxy- $\beta$ -tyrosyl-(*S*)-SgcC2 from 3-chloro-5-hydroxy- $\beta$ -tyrosine.

Finally, to determine that only (*S*)-3-chloro-5-hydroxy- $\beta$ -tyrosine was enantioselectively loaded to SgcC2 by SgcC1, the purified SgcC2-tethered  $\beta$ -amino acid product from the HiTrap Q (GE Healthcare) anion-exchange column described above was subjected to alkaline hydrolysis in 0.1 M KOH solution containing 50 mM DTT by incubating at 50  $^{\circ}$ C for 15 min. The resulting solution containing the free 3-chloro-5-hydroxy- $\beta$ -tyrosine was injected onto an Apollo C18 column (Grace Davison) by using a 20-min linear gradient from 0% to 25% B at a flow rate of 1 mL $\cdot$ min $^{-1}$  and UV-Vis detection at 283 nm for purification. The peak corresponding to 3-chloro-5-hydroxy- $\beta$ -tyrosine was collected, and the solution was dried using a speed-vac. The residue was redissolved in perchloric acid buffer (pH 1.5) and analyzed by using a chiral CrownPak CR (+) column (5  $\mu$ m, 150  $\times$  4.0 mm; Chiral Technologies Inc.). The column was developed under isocratic aqueous perchloric acid buffer (pH 1.5) at a flow rate of 1 mL $\cdot$ min $^{-1}$  as recommended by the manufacturer. With authentic (*S*)-3-chloro-5-hydroxy- $\beta$ -tyrosine and (*R*)-3-chloro-5-hydroxy- $\beta$ -tyrosine standards, the  $\beta$ -amino acid released was established to be (*S*)-3-chloro-5-hydroxy- $\beta$ -tyrosine (Fig. S3C), confirming the stereochemistry of the chemoenzymatically prepared (*S*)-3-chloro-5-hydroxy- $\beta$ -tyrosyl-(*S*)-SgcC2.

#### Time Course of SgcC5-Catalyzed Ester and Amide Bond Formation.

The time courses of SgcC5-catalyzed ester and amide bond formation were carried out in 200  $\mu$ L of reaction with 10 mM (*R*)-1-phenyl-1,2-ethanediol (structure **1a**), (*R*)-2-phenylglycinol (**3a**), and (*R*)-2-amino-1-phenyl-1-ethanol (**2a**) as acceptor substrates. The loading reactions (180  $\mu$ L) contained 100 mM Tris $\cdot$ HCl (pH 7.5), 200  $\mu$ M apo-SgcC2, 5 mM ATP, 1 mM CoA,

2 mM TCEP, 12.5 mM MgCl<sub>2</sub>, 5 mM 3-chloro-5-hydroxy- $\beta$ -tyrosine, 10  $\mu$ M Svp, and 10  $\mu$ M SgcC1 (final concentration for 200  $\mu$ L of reaction), and incubated at 25  $^{\circ}$ C for 45 min. After the acceptor substrates were added, the reactions were initiated by addition of SgcC5 (1  $\mu$ M For **1a**, 100  $\mu$ M for **2a**, and 20  $\mu$ M for **3a**) and carried out in duplicate. The reactions were quenched with 16% TFA at different time points (1, 2, 4, 8, 15, 30, 60, and 90 min for **1a**; 5, 10, 15, 30, 60, 90, and 180 min for **2a**; and 1, 2.5, 5, 10, 20, 40, 80, and 120 min for **3a**). After centrifugation, the clarified supernatant was analyzed by HPLC following the conditions described in the *Chemicals and Instruments* section. Under these conditions, **1b**, **1c**, **2b**, **3b**, and **3c** were eluted with retention times of 17.6 min, 18.2 min, 16.3 min, 15.5 min, and 16.6 min, respectively.

**Large-Scale Preparation, Purification, and Characterization of the Ester and Amide Products.** All products catalytically generated by SgcC5 were prepared chemoenzymatically and purified by HPLC equipped with a semipreparative Alltima C18 reverse-phase column (5  $\mu$ m, 250  $\times$  10 mm; Grace Davison) using a mobile phase gradient as follows: 0–20 min from 0% to 50% B, 20–21 min from 50% to 100% B, and 21–25 min at 100% B. Commercially available (*R*)-1-phenyl-1,2-ethanediol and (*R*)-2-phenylglycinol were used directly, but commercially available (*R*)-2-amino-1-phenyl-1-ethanol contains a significant amount of (*R*)-1-phenyl-1,2-ethanediol. To prepare pure (*R*)-2-amino-1-phenyl-1-ethanol, 200 mg of the commercial material was dissolved in water and acidified to pH 4. The resulting solution was loaded onto a preequilibrated cation-exchange column. After the column was washed with 300 mL of water, 5% ammonium hydroxide was used to elute the (*R*)-2-amino-1-phenyl-1-ethanol. After removal of solvent under reduced pressure, the resultant solid was redissolved in water and lyophilized to completely remove ammonium to afford pure (*R*)-2-amino-1-phenyl-1-ethanol.

**Esters **1b** and **1c**.** SgcC5-catalyzed scale-up preparation of ester product (**1b**) using (*R*)-1-phenyl-1,2-ethanediol (**1a**) as an acceptor substrate was achieved in a 10-mL reaction mixture containing 100 mM Tris $\cdot$ HCl (pH 7.8), 30 mM 3-chloro-5-hydroxy- $\beta$ -tyrosine, 30 mM ATP, 200  $\mu$ M apo-SgcC2, 1 mM CoA, 3 mM TCEP, 12.5 mM MgCl<sub>2</sub>, 10  $\mu$ M Svp, 10  $\mu$ M SgcC1, 30 mM (*R*)-1-phenyl-1,2-ethanediol, and 100  $\mu$ M SgcC5. The reaction mixture was shaken at 25  $^{\circ}$ C, and 5  $\mu$ M SgcC1 was added every 2 h, and 50  $\mu$ M SgcC5 was added every 4 h. The process of SgcC5-catalyzed large-scale reaction is depicted in Fig. S4. After 8 h, the reaction was quenched by 2 N HCl to precipitate all proteins, and the resulting supernatant was transferred to another tube, and the precipitate was washed with 5 mL of water 3 times. The water fractions were combined, and pH was adjusted to 7 with 1 N NaOH. The resulting solution was loaded onto a preequilibrated C18 Sep-pak cartridge (Waters), and the cartridge was washed with 20 mL of water. The crude products were eluted with 10 mL of acetonitrile. After removal of acetonitrile, the resultant solid was dissolved in water and purified by using a semipreparative HPLC column, yielding 6.4 mg of **1b** and 4.8 mg of **1c** that were obtained from spontaneous conversion of **1b**.

The equilibrium between **1b** and **1c** was established in a solution under the condition that was identical to the SgcC5 assays, except in the absence of SgcC5. An aliquot (25  $\mu$ L) was taken out and analyzed on HPLC every 30 min. HPLC analyses showed the spontaneous conversion reached an equilibrium after 90 min, on the basis of which the equilibrium constant was calculated.

The structures of **1b** and **1c** were elucidated by ESI-MS, 1D NMR, and 2D NMR. ESI-MS (*m/z*) for **1b**: [M + H]<sup>+</sup> found 352.1 and 354.1 (3:1), calcd 352.1 and 354.1 for C<sub>17</sub>H<sub>19</sub>ClNO<sub>5</sub>.

HR-ESI-MS ( $m/z$ ) for **1b**:  $[M + H]^+$  found 352.0952, calcd 352.0946 for  $C_{17}H_{19}ClNO_5$ . HR-ESI-MS ( $m/z$ ) for **1c**:  $[M + H]^+$  found 352.0946, calcd 352.0946 for  $C_{17}H_{19}ClNO_5$ . The NMR data are showed in Table 1.

**Amide 2b.** The SgcC5-catalyzed scale-up preparation of amide product (**2b**) using (*R*)-2-amino-1-phenyl-1-ethanol (**2a**) as an acceptor substrate was carried out in a 10-mL reaction that was identical to the reaction for preparation of **1b**, except that **2a** was substituted for **1a**. The purification of **2b** was achieved by a semipreparative HPLC chromatography, yielding 1.8 mg of **2b**. APCI-MS ( $m/z$ ):  $[M + H]^+$  found 351.1 and 353.1 (3:1), calcd 351.1 and 353.1 for  $C_{17}H_{19}ClN_2O_4$ . HR-MALDI-TOF-MS ( $m/z$ ):  $[M + Na]^+$  found 373.0920 and 375.0900, calcd 373.0926 and

375.0897 for  $C_{17}H_{18}ClN_2O_4Na$ . The NMR data (in  $CDCl_3/CD_3OD = 10/1$ ) are summarized in Table 2.

**Amide 3c.** The amide **3c** from the spontaneous conversion of SgcC5-formed ester product (**3b**) was obtained in the identical reaction condition, except that the reaction was performed in a 5-mL mixture, and **3a** was used as the acceptor substrate. HPLC chromatography yielded 0.3 mg of **3c**. HR-ESI-MS ( $m/z$ ):  $[M + H]^+$  found 351.1112 and 353.1089, calcd: 351.1106 and 353.1067 for  $C_{17}H_{19}ClN_2O_4$ .  $^1H$  NMR (500 MHz,  $CDCl_3/CD_3OD = 5:1$ ):  $\delta$  2.72 (dd,  $J = 15.6, 4.3$  Hz, 1H), 3.15 (overlapped with HDO), 3.71 (dd,  $J = 12.0, 9.5$  Hz, 1H), 3.79 (dd,  $J = 12.0, 4.5$  Hz, 1H), 4.41 (dd,  $J = 10.0, 4.5$  Hz, 1H), 5.05 (dd,  $J = 8.5, 4.5$  Hz, 1H), 6.83 (d,  $J = 2.0$  Hz, 1H), 6.97 (d,  $J = 2.0$  Hz, 1H), 7.22 (m, 2H), 7.31 (m, 3H).

1. Liu W, Christenson SD, Standage S, Shen B (2002) Biosynthesis of the enediyne antitumor antibiotic C-1027. *Science* 297:1170–1173.
2. Liu W, Shen B (2000) Genes for production of the enediyne antitumor antibiotic C-1027 in *Streptomyces globisporus* are clustered with the *cagA* gene that encodes the C-1027 apoprotein. *Antimicrob Agents Chemother* 44:382–392.
3. Lin S, VanLanen SG, Shen B (2007) Regiospecific chlorination of (*S*)- $\beta$ -tyrosyl-*S*-carrier protein catalyzed by SgcC3 in the biosynthesis of the enediyne antitumor antibiotic C-1027. *J Am Chem Soc* 129:12432–12438.
4. Lin S, Van Lanen SG, Shen B (2008) Characterization of the two-component, FAD-dependent monooxygenase SgcC that requires carrier protein-tethered substrates for the biosynthesis of the enediyne antitumor antibiotic C-1027. *J Am Chem Soc* 130:6616–6623.
5. Van Lanen SG, et al. (2005) Biosynthesis of the  $\beta$ -amino acid moiety of the enediyne antitumor antibiotic C-1027 featuring  $\beta$ -amino acyl-*S*-carrier protein intermediates. *J Am Chem Soc* 127:11594–11595.
6. Sánchez C, Du L, Edwards DJ, Toney MD, Shen B (2001) Cloning and characterization of a phosphopantetheinyl transferase from *Streptomyces verticillus* ATCC15003, the producer of the hybrid peptide-polyketide antitumor drug bleomycin. *Chem Biol* 8:725–738.
7. Saito F, Hori K, Kanda M, Kurotsu T, Saito Y (1994) Entire nucleotide sequence for *Bacillus brevis* Nagano Grs2 gene encoding gramicidin S synthetase 2: A multifunctional peptide synthetase. *J Biochem* 116:357–367.
8. Mootz HD, Marahiel MA (1997) The tyrocidine biosynthesis operon of *Bacillus brevis*: Complete nucleotide sequence and biochemical characterization of functional internal adenylation domains. *J Bacteriol* 179:6843–6850.
9. Motamedi H, Shafiee A (1998) The biosynthetic gene cluster for macrolactone ring of the immunosuppressant FK506. *Eur J Chem* 256:528–534.
10. Schwecke T, et al. (1995) The biosynthetic gene cluster for the polyketide immunosuppressant rapamycin. *Proc Natl Acad Sci USA* 92:7839–7843.
11. Ehmann DE, Shaw-Reid CA, Losey HC, Walsh CT (2000) The EntF and EntE adenylation domains of *Escherichia coli* enterobactin synthetase: Sequestration and selectivity in acyl-AMP transfers to thiolation domain cosubstrates. *Proc Natl Acad Sci USA* 97:2509–2514.
12. Keating TA, Marshall CG, Walsh CT, Keating AE (2002) The structure of VibH represents nonribosomal peptide synthetase condensation, cyclization and epimerization domains. *Nat Struct Mol Biol* 9:522–526.
13. Keating TA, Marshall CG, Walsh CT (2000) Reconstitution and characterization of the *Vibrio cholerae* vibriobactin synthetase from VibB, VibE, VibF, and VibH. *Biochemistry* 39:15522–15530.
14. Ehling-Schulz M, et al. (2005) Identification and partial characterization of the nonribosomal peptide synthetase gene responsible for cereulide production in emetic *Bacillus cereus*. *Appl Environ Microbiol* 71:105–113.
15. Magarvey NA, et al. (2006) Biosynthetic characterization and chemoenzymatic assembly of the cryptophycins. Potent anticancer agents from *Nostocyanobionts*. *ACS Chem Biol* 1:766–779.
16. Fujimori DG, et al. (2007) Cloning and characterization of the biosynthetic gene cluster for kutznerides. *Proc Natl Acad Sci USA* 104:16498–16503.
17. Cheng YQ (2006) Deciphering the biosynthetic codes for the potent Anti-SARS-CoV cyclodepsipeptide valinomycin in *Streptomyces tsusimaensis* ATCC 15141. *ChemBiochem* 7:471–477.
18. Zaleta-Rivera K, et al. (2006) A bidomain nonribosomal peptide synthetase encoded by FUM14 catalyzes the formation of tricarballic esters in the biosynthesis of fumonisins. *Biochemistry* 45:2561–2569.
19. Samel SA, Schoenafinger G, Knappe TA, Marahiel MA, Essen LO (2007) Structural and functional insights into a peptide bond-forming bidomain from a nonribosomal peptide synthetase. *Structure* 15:781–792.
20. Tanovic A, Samel SA, Essen LO, Marahiel MA (2008) Crystal structure of the termination module of a nonribosomal peptide synthetase. *Science* 321:659–663.

SgcC5 155-DAVLVLI**AHHTAAD**AWAMHVIARDLLNL**YAARRG**-188  
 GrsB 138-NYQMIWSF**HHILMD**GWCFNIIFNDLFNI**YLSLKE**-173  
 TyrB 138-DYQVIWSF**HHILMD**GWCFSIIFD DLLAI**YLSLQN**-173  
 SrfA-C 138-SFEWVWSY**HHIILD**GWCFGIIVVQDLFKV**YNALRE**-173  
 VLM1 3018-EHVFAFSF**PHVSLD**GWSVFRILARTLEL**YDAGVP**-3051  
 Cesa 2971-EYELIWSF**HHISID**GWSIFLVLSEVVA**YKQLIQ**-3006  
 RapPC2 1218-DHILILML**HHIAGD**GWSFDVLRVRELSAL**YAECRV**-1251  
 FkbPC1 149-DHVLAVTV**HHVAGD**GWSFGLLQHELA**HYTALRD**-182  
 RapPC1 159-DHVLALTV**HHIAGD**GWSLAILRMELSAQ**YAPLLR**-192  
 CrpD 1266-EYVLLLT**MHHIVSD**GWSMGIFSQELSTL**YQAFSA**-1299  
 TyrC-C6 213-RYVLF**TDMHHSISD**GVSSGILLAE**WVQLYQG**----242  
 KtzE 1237-RAELVLSA**HHALFD**GWSEPLIARDLL**GHYGRRHA**-1261  
 EntF 129-RWYWYQRY**HHLLVD**GFSFPAITRQIANI**YCTWLR**-162  
 VibH 117-EHLIY**TRAHHIVLD**GYGMMLFEQRLSQ**HYQSLLS**-150  
 VibF 2075-TQYLSLLF**HHIVLDE**WSINILMDELAQ**VYQHSVQ**-2108  
 FkbPC2 1201-DHVL**LLMLHHLAGD**GWSFDLLVRELSG--TQPDL-1233  
 FUM14p 236-QNFFVISL**DHTHCD**AFSRYLIDKEILQILKQ**PTE**-270

**Fig. S1.** Sequence alignment of putative active site region for SgcC5 with other condensation enzymes, including GrsB, the first C domain in the biosynthesis of gramicidin S (accession number: POC064) (7), TyrB, the first C domain in the biosynthesis of tyromycin (accession number: O30408) (8), FkbP (accession number: AAF86395) (9), RapP (accession number: CAA60461) (10), EntF (accession number: P11454) (11), VibH (accession number: AAD48879) (12), VibF (accession number: AAG00566) (13), Cesa (accession number: ABD14711) (14), CrpD (accession number: ABM21572) (15), KtzE (accession number: ABV56585) (16), VLM1 (accession number: ABA59547) (17), and FUM14P (accession number: AAN74817) (18), TyrC-C6 (accession number: 2JGP\_A) (19), and SrfA-C (accession number: 2VSQ\_A) (20).

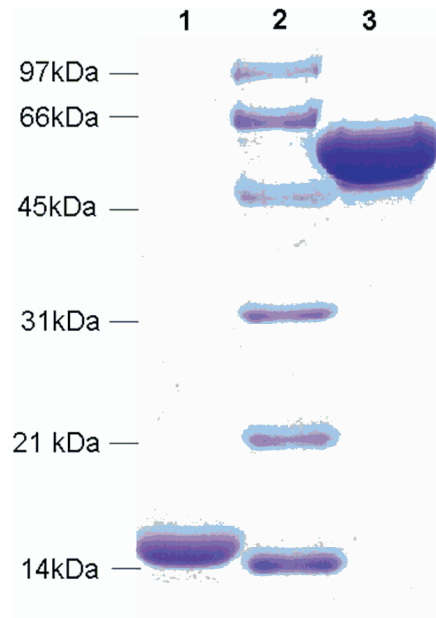
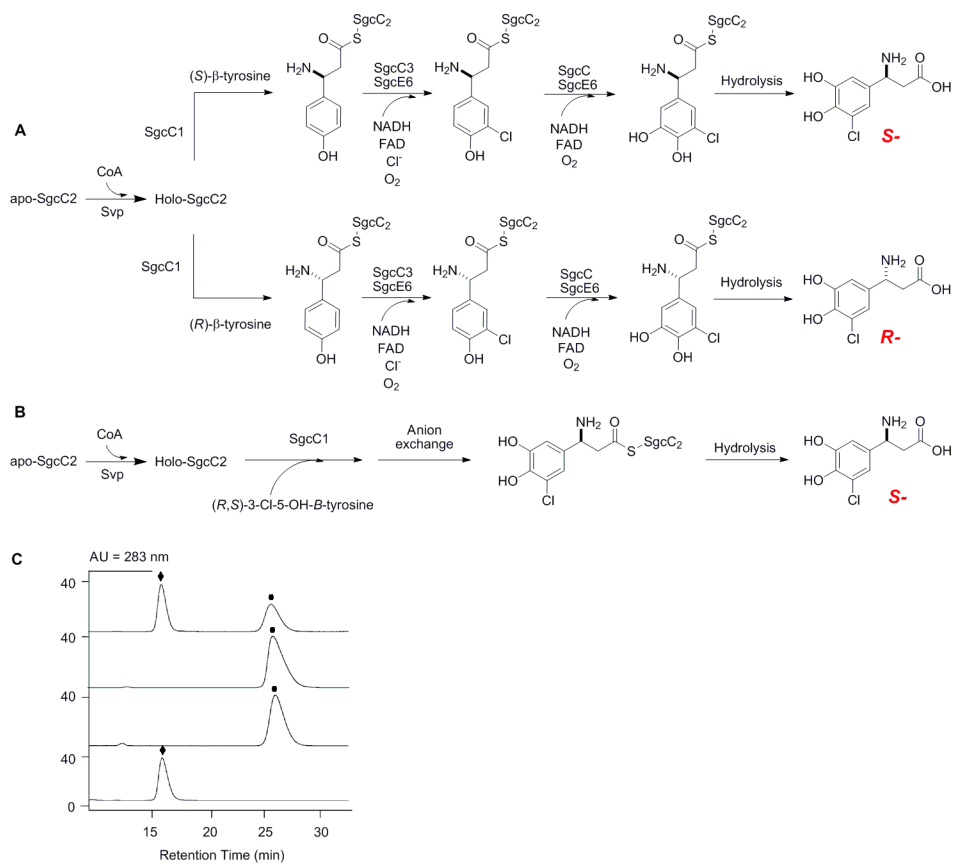
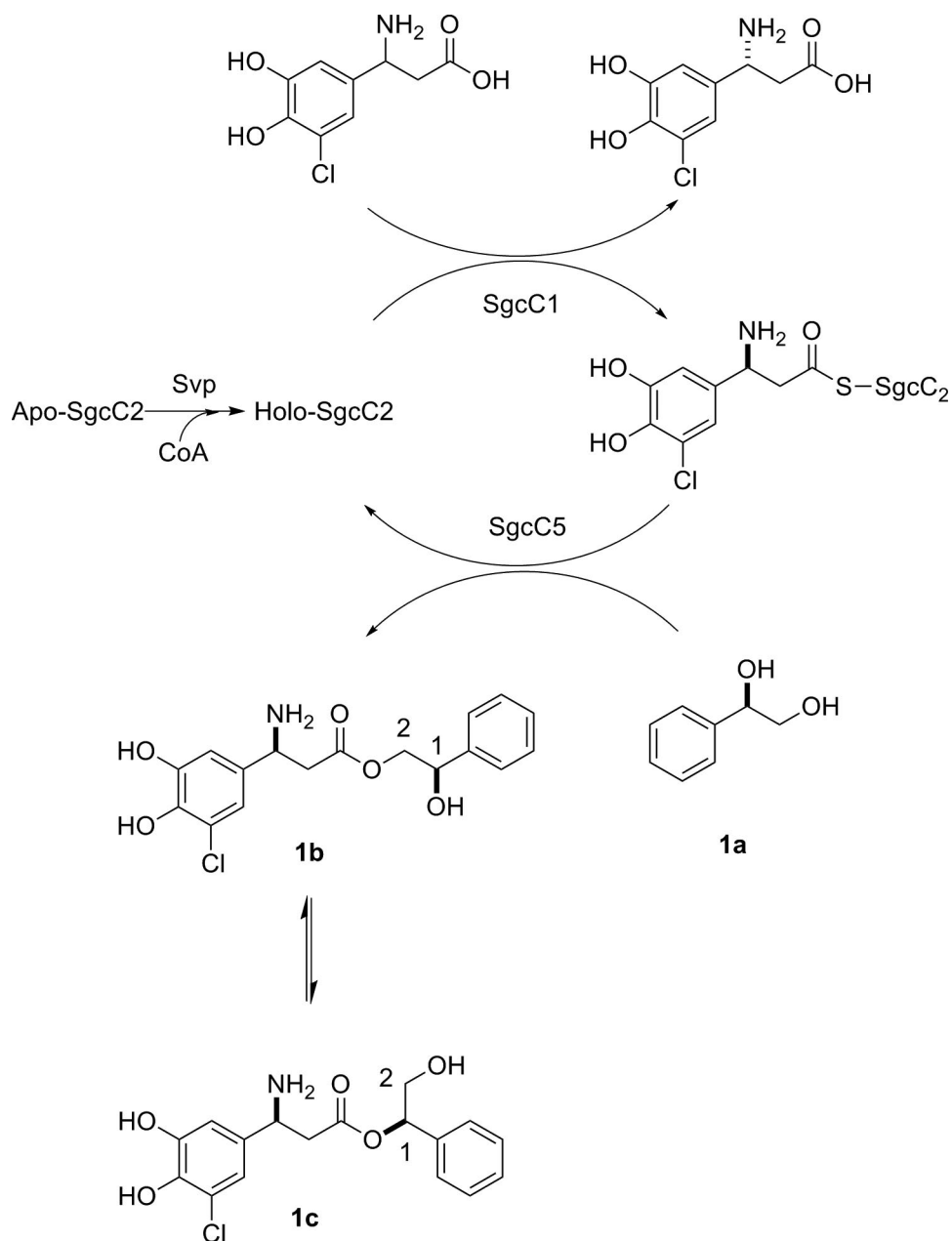


Fig. S2. SDS/PAGE of purified proteins: lane 1, SgcC2; lane 2, low-range protein MW standards; lane 3, SgcC5.



**Fig. S3.** (A) Chemoenzymatic synthesis of (R)-3-chloro-5-hydroxy-β-tyrosine and (S)-3-chloro-5-hydroxy-β-tyrosine standards from (R)-β-tyrosine and (S)-β-tyrosine, respectively, via sequential C-3 chlorination by SgcC3, C-5 hydroxylation by SgcE6, and finally, alkaline hydrolysis. (B) Chemoenzymatic synthesis of (S)-3-chloro-5-hydroxy-β-tyrosyl-(S)-SgcC2 from (S)-3-chloro-5-hydroxy-β-tyrosine. (C) Stereochemistry determination of enantiospecific loading of (S)-3-chloro-5-hydroxy-β-tyrosine (●) to SgcC2 with enzymatically synthesized (R)-3-chloro-5-hydroxy-β-tyrosine (◆) and (S)-3-chloro-5-hydroxy-β-tyrosine (●) standards by chiral HPLC: (i) synthetic racemic 3-chloro-5-hydroxy-β-tyrosine standard, (ii) (S)-3-chloro-5-hydroxy-β-tyrosine released from the chemoenzymatically prepared 3-chloro-5-hydroxy-β-tyrosyl-(S)-SgcC2 donor substrate for SgcC5, (iii) (S)-3-chloro-5-hydroxy-β-tyrosine standard prepared from the enzymatic C-5 hydroxylation and C-3 chlorination of (S)-β-tyrosyl-(S)-SgcC2, and (iv) (R)-3-chloro-5-hydroxy-β-tyrosine standard prepared from the enzymatic C-5 hydroxylation and C-3 chlorination of (R)-β-tyrosyl-(S)-SgcC2.



**Fig. S4.** Scheme depicting large-scale enzymatic preparation of ester **1b** from 3-chloro-5-hydroxy- $\beta$ -tyrosine by Svp-, SgcC1-, and SgcC2-mediated synthesis of (S)-3-chloro-5-hydroxy- $\beta$ -tyrosyl-(S)-SgcC2 in situ and SgcC5-catalyzed subsequent ester formation between (S)-3-chloro-5-hydroxy- $\beta$ -tyrosyl-(S)-SgcC2 and (R)-1-phenyl-1,2-ethanediol (**1a**), as well as spontaneous conversion between **1b** and **1c** via a 1,2-acyl migration.

**Table S1. NMR data (in D<sub>2</sub>O) for 1b and 1c**

<sup>1</sup> H-NMR (500 MHz, δ)	<sup>13</sup> C-NMR (125 MHz, δ)
<b>1b</b>	
3.10 (dd, <i>J</i> = 16.0, 8.0 Hz, 1H, H $\alpha$ )	38.1 (C- $\alpha$ )
3.16 (dd, <i>J</i> = 16.5, 6.0 Hz, 1H, H $\alpha$ )	51.0 (C- $\beta$ )
4.33 (m, 2H, H $\beta'$ )	68.9 (C- $\beta'$ )
4.61 (dd, <i>J</i> = 8.0, 6.0 Hz, 1H, H $\beta$ )	71.3 (C- $\alpha'$ )
4.92 (t, <i>J</i> = 5.5 Hz, 1H, H $\alpha'$ )	113.6 (C-6)
6.86 (d, <i>J</i> = 2.0 Hz, 1H, H-6)	120.2 (C-2)
6.97 (d, <i>J</i> = 2.0 Hz, 1H, H-2)	121.8 (C-3)
7.33 (d, <i>J</i> = 7.5 Hz, 2H, H-2'/6')	126.5 (C-2'/6')
7.39 (m, 3H, H-3'/4'/5')	127.9 (C-1)
	128.6 (C-4')
	128.9 (C-3'/5')
	139.7 (C-1')
	142.0 (C-4)
	146.2 (C-5)
	171.0 (C=O)
<b>1c</b>	
3.20 (d, <i>J</i> = 8.4 Hz, 1H, H $\beta'$ )	38.7 (C- $\alpha$ )
3.72 (dd, <i>J</i> = 12.4, 4.0 Hz, 1H, H $\alpha$ )	51.7 (C- $\beta$ )
3.78 (dd, <i>J</i> = 12.4, 7.2 Hz, 1H, H $\alpha$ )	64.1 (C- $\beta'$ )
4.49 (t, <i>J</i> = 8.2 Hz, 1H, H $\beta$ )	78.5 (C- $\alpha'$ )
5.60 (dd, <i>J</i> = 7.6, 3.6 Hz, 1H, H $\alpha'$ )	113.7 (C-6)
6.78 (d, <i>J</i> = 2.0 Hz, 1H, H-6)	120.6 (C-2)
6.91 (d, <i>J</i> = 2.0 Hz, 1H, H-2)	121.7 (C-3)
6.97 (d, <i>J</i> = 7.2 Hz, 2H, H-2'/6')	126.5 (C-2'/6')
7.20–7.28 (m, 3H, H-3'/4'/5')	127.9 (C-1)
	128.7 (C-3'/5')
	128.8 (C-4')
	136.3 (C-1')
	142.0 (C-4)
	146.2 (C-5)
	170.8 (C=O)



**Table S2. NMR data for 2b**

<sup>1</sup> H-NMR (500 MHz, δ)	<sup>13</sup> C-NMR(125 MHz, δ)
2.71 (dd, <i>J</i> = 15.6, 4.2 Hz, 1H, H $\alpha$ )	40.0 (C- $\alpha$ )
3.06 (dd, <i>J</i> = 15.4, 10.5 Hz, 1H, H $\alpha$ )	52.8 (C- $\beta$ )
3.41 (dd, <i>J</i> = 13.9, 2.9 Hz, 1H, H $\beta'$ )	47.3 (C- $\beta'$ )
3.59 (dd, <i>J</i> = 13.9, 9.3 Hz, 1H, H $\beta'$ )	73.3 (C- $\alpha'$ )
4.48 (dd, <i>J</i> = 10.3, 3.9 Hz, 1H, H $\beta$ )	111.5 (C-6)
4.76 (dd, <i>J</i> = 9.5, 3.1 Hz, 1H, H $\alpha'$ )	120.0 (C-2)
6.86 (dd, <i>J</i> = 2.0 Hz, 1H, H6)	120.4 (C-3)
7.00 (dd, <i>J</i> = 1.7 Hz, 1H, H2)	126.0 (C-2'/6')
7.31 (m, 2H, H2'/6')	127.6 (C-1)
7.38 (m, 3H, H3'/4'/5')	128.2 (C-4')
	128.8 (C-3'/5')
	141.5 (C-1')
	142.7 (C-4)
	146.4 (C-5)
	170.9 (C=O)